Inertia Response Improvement in AC Microgrids: A Fuzzy-Based Virtual Synchronous Generator Control

Amin Karimi, Yousef Khayat, *Student Member, IEEE*, Mobin Naderi, *Student Member, IEEE*, Tomislav Dragičević, *Senior Member, IEEE*, Rahmatollah Mirzaei, Frede Blaabjerg, *Fellow, IEEE*, and Hassan Bevrani, *Senior Member, IEEE*

***Abstract*—The absence of rotational masses from synchronous generators in converter-interfaced microgrids leads to a lack of inertia. Consequently, the system exhibits steeper frequency variations and higher frequency nadir, which may degrade the dynamic performance and challenge the operation of sensitive equipment such as protective relays in the grid. Virtual synchronous generator is introduced as an effective solution to increase the inertial response of converter interfaced renewable energy sources. This article proposed a fuzzy controller, which is augmented on the virtual synchronous generator topology to damp the perturbation during transients by increasing the inertia of the system. The proposed fuzzy control adds a correction term to the governor's output power that increases the system inertia during transients. In order to compare the inertial response improvement, a comparison between proposed fuzzy control technique and cost function based inertia and damping coefficient optimization is done on a virtual synchronous generator platform. It is shown that online measurement based adaptive methods have a better inertial response against other time-consuming techniques. To further verification, a number of experiments are done, which confirm the merits of the proposed fuzzy based virtual synchronous generator control method.**

***Index Terms*—AC microgrids, converter interfaced generation, frequency stability, transient performance, virtual inertia, virtual synchronous generator.**

I. Introduction

MICROGRIDS and their flexible control features propose a practical solution to employ better renewable energy resources by converter interface power electronics [1]. On the other hand, lack of synchronous generators in the converter interfaced microgrids (MGs) leave more operation-protection consequences. Though, low inertia of converter interfaced renewable energy sources (CIRESs) are introduced as a general drawback, they have fast controllable dynamics, which may be introduced as promising solutions for both power support and frequency response reaction [2].

In order to improve the system stability and prevent them from triggering the sensitive protection relays, performance requirements are needed to increase the inertia response of the CIRES-based MGs [3], [4].

The concept of virtual synchronous generator (VSG) is proposed to increase the inertia of the MGs by emulating the behavior of synchronous generator (SG) [5], [6]. A well-known objective of VSGs is stated by employing CIRESs in the same way as synchronous generators. By this, the well-established operation-protection methods for conventional power systems can be used for MGs with a high penetration level of CIRESs [7].

According to the ac MG operation modes, i.e., autonomous and grid connected, CIRESs can be categorized into grid-forming, grid-feeding, and grid-supporting power converters [8]. The grid-forming CIRESs can just be operated in the autonomous mode in order to form voltage sources with certain frequency and voltage amplitude. The grid-feeding CIRESs can be used in both autonomous and grid-connected modes for the sake of supplying active and reactive powers. However, in the islanded MGs, at least one grid-forming CIRES is required in parallel. Note that the grid-feeding CIRESs are not able to contribute in voltage/frequency regulation. The grid-supporting CIRESs are operated as both current and voltage sources. Although the current source grid-supporting CIRESs can be operated in the grid-connected mode unconditionally, they cannot be used independently in the autonomous mode. Nevertheless, the voltage source grid-supporting CIRESs are able to work in both modes. Generally, the grid-supporting CIRESs contribute to supply active/reactive power and also voltage/frequency regulation. Therefore, they are much more flexible for supplementary control services, e.g. improving inertia response and mitigating power fluctuations. The VSG control strategy is a type of grid-supporting CIRESs.

The VSG-based grid-supporting CIRESs are allowed to be the active components to support the frequency dynamics and the role of inertia response will be performed by them. In these CIRESs, the oscillations on the output power and frequency may easily occur due to the high fluctuations of the distributed generations. To address this problem, several control methods have been designed to suppress the frequency and active power oscillations [9]. By adjusting the inertia and/or

Manuscript received April 1, 2019; revised June 25, 2019; accepted August 8, 2019. Date of publication August 25, 2019; date of current version January 10, 2020. This work was supported by the Energy Department, Aalborg University, for the SMGRC Visiting Researchers. Recommended for publication by Associate Editor A. Davoudi. *(Corresponding author: Yousef Khayat.)*

A. Karimi, Y. Khayat, M. Naderi, R. Mirzaei, and H. Bevrani are with the Smart/Micro Grids Research Center, University of Kurdistan, Sanandaj 66177-15175, Iran (e-mail: a.karimi@eng.uok.ac.ir; y.khayat@eng.uok.ac.ir; m.naderi@eng.uok.ac.ir; r.mirzaee@uok.ac.ir; bevrani@eng.uok.ac.ir).

T. Dragičević and F. Blaabjerg are with the Department of Energy Technology, Aalborg University, 9220 Aalborg, Denmark (e-mail: tdr@et.aau.dk; fbl@et.aau.dk).

Color versions of one or more of the figures in this article are available online at http://ieeexplore.ieee.org.

Digital Object Identifier 10.1109/TPEL.2019.2937397

the damping coefficients of VSGs, the output oscillations and the VSG behavior can be changed directly. In order to better understand the VSG parameter design, small-signal modeling is done in [10], where the inertia and damping coefficients of the VSG can be determined more accurately. A modeling study is presented in [11], where the influences of parameter variation and perturbation effects on the active power and frequency oscillations for a VSG are studied by proposing the small-signal model and illustrating the dynamic performances in detail. A virtual capacitor algorithm to enhance the reactive power sharing in VSG-based MGs in [12] and an adaptive linear quadratic regulator-based VSG in [13] to improve the inertial response of the system have also been presented.

From the inner loops architecture point of view, the VSG-based CIRESs can be classified into two categories [14]: 1) without current control loop [15], [16], and 2) with current control loop [17]. The first category suffers from short-circuit faults since there is not a current control loop in the converter control framework. The VSGs belonging to the second category, which includes the current controller to enable the control of grid current and enhance the converter with fault ride through capability. This control approach supplements the outer control loop of a vector controlled converter without modifying the structure of the overall system. It is worth to note that the current control is necessary for the LCL-filtered converter structure [18].

As presented in [19], a self-adaptive VSG control method based on RoCoF, and in [20] a self-tuning-based algorithm were employed to continuously optimize the virtual inertia among predefined inertia moment J and damping coefficient D in order to minimize the frequency deviation and output power oscillation of the VSG. Similar methods are addressed in [21] and [22], where different values of J and D were employed to improve the dynamics of frequency response. In [23] and [24], by changing droop gain as a function of frequency and frequency variation an improved virtual inertia response is obtained. Zhang *et al.* [25] proposed a fuzzy control to improve the frequency response of a wind turbine system, which needs a detailed model on pitch angle control, wind storage system, and wind speed. From a practical point of view, the relationship between the inertia response and dc-link energy as well as other design parameters are addressed in [26]. Inspired by the VSG functions on the flexible ac transmission system, Karimi *et al.* [27] have improved the inertial response of CIRES-based MGs by employing the STATCOM functions into the VSGs.

In this article, by employing a fuzzy controller (FC), which is used in the VSG control platform, named FC-VSG, the inertial response of CIRES-based VSGs can be improved. In both grid connected and autonomous modes of ac MGs and, in addition, the active power performance in the transient state is enhanced. The designed FC generates a correction term, which is added to the governor's output power, i.e., input power of the swing equation, to improve the VSG performance in order to increase the system inertia during transients, with a small computational burden. It is implemented by a set of logic membership functions in transient states. The proposed FC makes the VSG response more applicable for practical implementations, since it employs three main effective parameters related to inertial response, i.e., the rotating angle change $\Delta\delta$, the MG frequency ω and the RoCoF. The proposed FC-VSG has the following advantages over the existing methods.

1) In this article, $\Delta\delta$, ω, and $\dot{\omega}$ (RoCoF) are employed by an FC to improve the inertial response. Meanwhile, the existing results in [21]–[24] are only working on the tuning of the VSG parameters (J and D) by using optimization methods. These approaches are not fast enough to leave their impact on inertial response due to their computations.
2) Comparing with the existing tuning or gain scheduling methods in [19] and [20], this article utilizes an FC representation, which is merged with a VSG scheme to provide a novel nonlinear inertial response improvement by modifying the governor's output power using low online computational burden.
3) Comparing with the existing inertia response improvement approach in [27], the proposed FC can compensate the inertia and transient oscillations continuously, while [27] improves the inertia response by a bang–bang control method. The proposed FC rapidly adjusts the prime mover power of the governor to improve the inertia response.

The rest of this article is organized as follows. In Section II, common CIRES control methods and their role in order to provide a sufficient level of inertia for the system are discussed. Section III presents a nonlinear model of a VSG connected to an equivalent Thevenin model of a weak grid or an MG. The proposed FC controller with its membership functions and design procedure are presented in Section IV. In Section V, the effect of online measurement control FC-VSG with direct search methods to tune the inertia and damping coefficients is compared by simulations. Verification by experimental tests are performed in Section V. Finally, concluding remarks and future works are outlined in Section VI.

II. Inertia Support Necessity for Grid-Connected CIRESs

Increasing the inertia response in power systems with a high penetration of CIRES is possible by implementing virtual inertia algorithms in the power electronics devices, so they mimic the inertial response of the synchronous generators. As mentioned previously, the two most common solutions to connect a CIRES are grid-feeding and grid-supporting operation. The grid-feeding configuration is designed to inject power proportional to the frequency deviation and the RoCoF, which are measured by a phase-locked loop (PLL). On the other hand, the grid-supporting configuration responds to the power fluctuations by changing the frequency based on a droop characteristics or swing equation of the synchronous generators.

It is worth to note that a number of synchronous machines may be disconnected when the renewable generation units produce their expected production in a favor weather. A real-life report on the system's inertia variability is presented in [28], which shows the time-variant German power system inertia for the year 2012. It is reported that the total system inertia only for the cases that electric energy is generated by synchronous generation machines is 6 s, but when the penetration level of the CIRESs

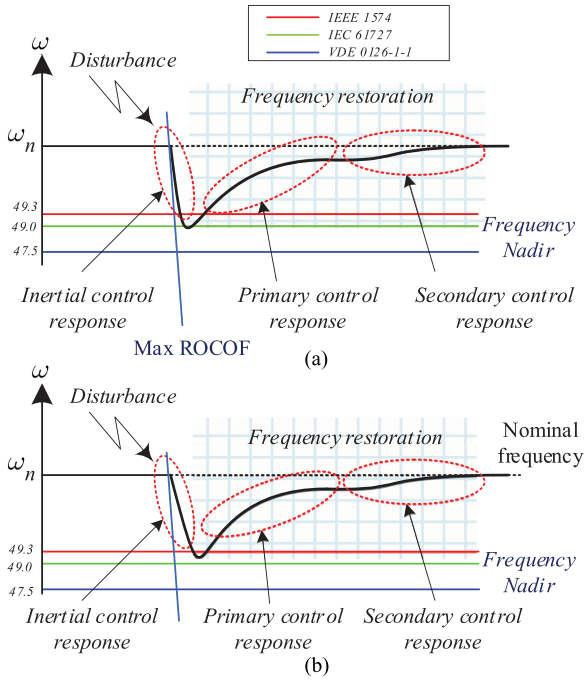

Fig. 1. Frequency response to a disturbance such as intentional/unintentional islanding, faults, and load changes. (a) Low inertial CIRES-based power system. (b) Large inertial system (rotating-mass conventional power system).

is increased, the inertia constant of the system is easily reduced to 3 s.

By increasing the penetration level of CIRESs and replacement instead of synchronous machines, the system inertia becomes a stochastic and time-dependent variable as a function of the expected wind and solar power output. Hence, the system inertia is increasingly becoming a stochastic variable subject to a significant level of variability and dependent on weather conditions. More importantly, situations may emerge when the power electronics based power system is not able to provide inertia support or provide an acceptable inertial response. Technical reports [29]–[31] have discussed this challenge. A possible solution to provide a sufficient level of inertia independent from the CIRES capacity is remodeling the system inertia as a time-dependent stochastic variable that needs to be considered as an uncertain variable into the dispatch and robustness analysis and modeling. Robust analysis and modeling either by conservative modeling such as unstructured or parametric uncertainty or lower conservative approaches such as unstructured uncertainty modeling will be promising solutions to the inertia issues.

The necessity of an accurate modeling of power electronics converters, their control layers and limitations focusing on the short time scales is required to analyze and propose new solutions to provide the inertia level of the system.

Fig. 1 shows a conceptual frequency response of a CIRES-based power system [see Fig. 1(a)], and large inertia system (rotating-mass conventional power system) [see Fig. 1(b)] after a disturbance. The frequency dynamics are addressed in many power system text books, for example [1, Ch. 12] or [2, Ch. 8]. As illustrated in Fig. 1, the frequency dynamics includes two parts: 1) inertial response once a disturbance occurs, and

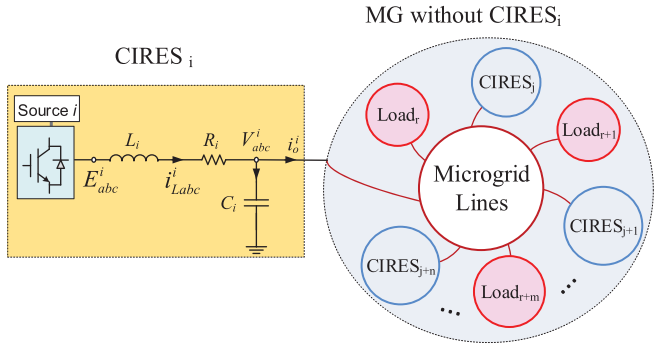

Fig. 2. General diagram of a very weak grid (MG) with focus on CIRES$_i$ as a VSG.

2) frequency restoring control, which are performed by the primary and secondary control layers. The inertia response is expressed using two common indices, i.e., RoCoF and the frequency Nadir [20], which are also shown in Fig. 1. The lower RoCoF and frequency nadir means more improved inertia response [20].

III. VSG Modeling

A VSG can be connected to a strong grid, weak grid, or an islanded MG (as a very weak grid). It is worth to mention that the strong grid can be modeled as an ideal voltage source, while in the real grids the grid impedance Z_g should be included as a metric of the grid strength/weakness as follows [14]:

$$\text{SCR} = \frac{1}{Z_g(\text{p.u.})} \tag{1}$$

where the short-circuit ratio (SCR) for strong grids is larger than 3, for weak grids its value is between 2 and 3, and for very weak grids, it is less than 2 [14]. In the case of islanded MGs fully based on CIRESs, the well-known current limiting function embedded in inner current controllers does not permit an SCR larger than one. Therefore, Z_g should be considered precisely in this article. To this end, an equivalent Thevenin model of an MG as a special challenging weak grid with variable inertia and damping coefficients is presented in the following section.

In the following, we try to present a parametric model of a VSG connected to an equivalent Thevenin model with equivalent voltage $E_{\text{th}} = |E_{\text{th}}|\angle\theta_{\text{th}}$ and equivalent impedance Z_{th}.

A. Equivalent Thevenin Based Model of MG Power Side

The presented MG modeling in [32], also called static Z_{th} modeling, is employed here to simplify the rest of islanded MG connected to a VSG. A conceptual diagram of an islanded MG in a general case is shown in Fig. 2, where the focus is on a single-line diagram of the CIRES$_i$. As mentioned, the CIRES$_i$ is controlled as a VSG and its dc-link voltage is assumed to be constant [33]. The rest of the MG includes other CIRESs, loads, and lines, while they are electrically linked. The other CIRESs are operated in the form of being grid forming [8]. Here, we aim to find a model for the MG power side. To achieve this goal, the CIRES power part including a dependent voltage source and an RLC filter are modeled in details, and the effects of the rest of

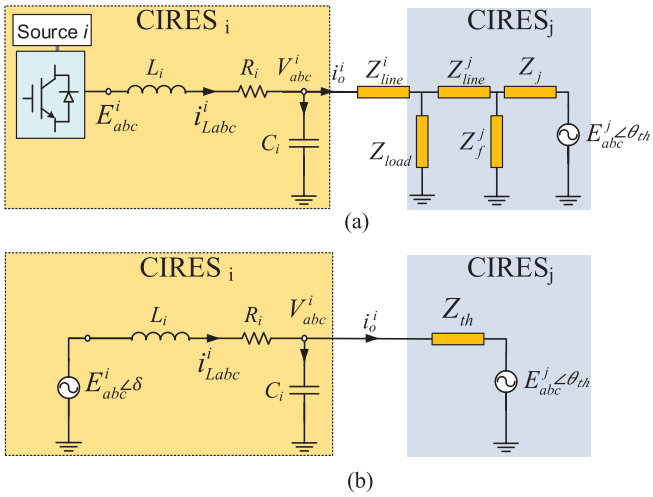

Fig. 3. CIRES$_i$ model. (a) Typical two CIRES based MG with lines and loads. (b) Equivalent of the system from a CIRES$_i$ point of view.

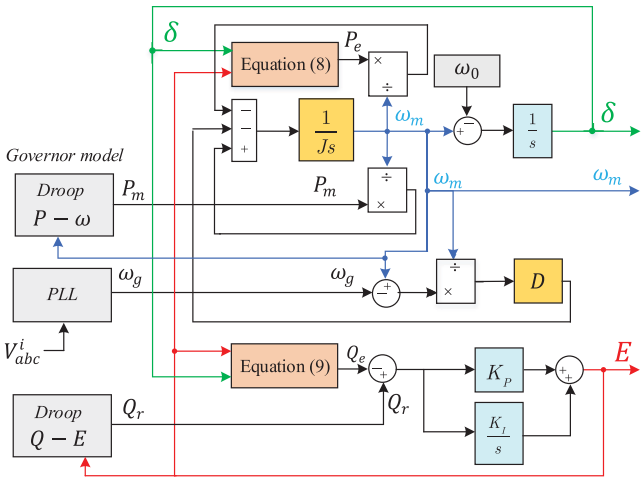

Fig. 4. Dynamics of a VSG-based CIRES connected to a weak grid.

MG on the CIRES$_i$ are considered in the form of an equivalent Thevenin circuit.

Fig. 3(a) shows the MG model having a voltage source representing the inverter, filter inductance, capacitance, resistances, and a Thevenin equivalent circuit. In this electrical model, the Thevenin equivalent is composed of an impedance equivalent to all other impedances in the MG including lines, loads, and CIRES filters, and the impact of all other CIRESs coupled at PCC with CIRES$_i$ is shown with a voltage source equivalent. Three-phase equations in the *abc*-frame are as follows:

$$E^i_{abc} = R_i i^i_{Labc} + L_i \frac{d}{dt} i^i_{Labc} + V^i_{abc} \tag{2}$$

$$i^i_{Cabc} = i^i_{Labc} - i^i_{Oabc} = C^i_f \frac{d}{dt} V^i_{abc} \tag{3}$$

$$V^i_{abc} = Z^i_{\text{th}} i^i_{Oabc} + E^i_{\text{th}} \tag{4}$$

where Z^i_{th} and E^i_{th} are calculated easily according to the structure of the rest of MG. In the case of two-CIRES MG as shown in Fig. 3(b), Z^i_{th} and E^i_{th} are obtained as

$$\begin{cases} Z_{\text{th}} = Z^1_{\text{line}} + Z_{\text{load}} || \left(Z^2_{\text{line}} + Z_2 || Z^2_f \right) \\ E_{\text{th}} = \left(\dfrac{(Z_2 || Z^2_f)(Z_{\text{load}} || (Z^2_{\text{line}} + Z_2 || Z^2_f))}{Z_2 (Z^2_{\text{line}} + Z_2 || Z^2_f)} \right) E^2_{\text{an}} \angle \theta_2 \end{cases} \tag{5}$$

where all impedances can be observed in Fig. 3(a), E^2_{an} and θ_2 are the voltage amplitude and phase angle of CIRES$_2$ being in the equilibrium point.

B. Nonlinear Behavior of VSG

Fig. 4 illustrates the topology and control platform of the VSG. It is realized by implementing the virtual swing equation, which employing active and reactive power droops on the output powers of the CIRES. It can be connected to a weak grid or a very weak grid, e.g., an MG, through an LC filter and the grid impedance Z_{th}.

The well-known inertia equation, which illustrates the dynamics of the synchronous generators is given as

$$\dot{\delta} = \omega_m - \omega_0 \tag{6}$$

$$J \omega_m \dot{\omega_m} = P_m - P_e - D(\omega_m - \omega_g) \tag{7}$$

where δ is the VSG voltage angle, ω_m is the angular frequency of the VSG, ω_g is the measured angular frequency through the PLL, J is the virtual moment of inertia, D is the damping coefficient, and P_m is the governor's output power. The active and reactive power injected to the grid can be calculated based on the electrical part modeling, as shown in Fig. 3(b), as follows:

$$P_e = Y_{\text{th}}(V^2 \cos \varphi_{\text{th}} - V|E_{\text{th}}| \cos(\vartheta + \varphi_{\text{th}})) \tag{8}$$

$$Q_e = Y_{\text{th}}(V^2 \sin \varphi_{\text{th}} - V|E_{\text{th}}| \sin(\vartheta + \varphi_{\text{th}})). \tag{9}$$

where $Y_{\text{th}} = |Z^{-1}_{\text{th}}|$, $\varphi_{\text{th}} = \angle Z_{\text{th}}$, V is the RMS value of the V^i_{abc}, and $\vartheta = \delta - \theta_{\text{th}}$. Z_{th}, φ_{th} and θ_{th} are calculated according to the equivalent Thevenin circuit model presented in the previous section.

The output voltage of the VSG is controlled by a proportional-integral (PI) controller with the following dynamics:

$$E = \left(K_P + \frac{K_I}{s} \right) (Q_r - Q_e) \tag{10}$$

where K_P and K_I are the proportional and integral gains of the PI voltage controller. In order to find the voltage dynamics, (10) can be rewritten as

$$\dot{E} = K_P \dot{Q}_r - K_P \dot{Q}_e + K_I (Q_r - Q_e) \tag{11}$$

where the term $\dot{Q}_r$ is related to the dynamics of the measured voltage (V), which can be neglected with respect to the frequency dynamics [1]. Consequently, the voltage dynamics (12) can be represented as

$$\dot{E} = -K_P \dot{Q}_e + K_I (Q_r - Q_e). \tag{12}$$

To complete the modeling of the VSG, the governor model should be included as

$$P_m = P_0 - k_p(\omega_0 - \omega_m). \tag{13}$$

Finally, (6)–(9), (12), and (13) present the nonlinear dynamics of a VSG. Obviously, the nonlinear behavior of the VSG connected to a weak grid can be observed based on (7)–(9). Therefore, employing a nonlinear controller such as an FC technique handles these nonlinearities and improves the performance of the VSG.

IV. Fuzzy Logic Controller Implementation

One way to cope with a nonlinear feature of the physical-dynamical systems is to represent a nonlinear model including a number of differential equations, which are simple and understandable for their respective subdomains. Facing nonlinear and complex systems, it should be recognized that the modeling has a key role and it is important to realize the system modeling, behavior, and system operation points in various conditions.

The concept of fuzzy systems presents powerful control techniques to cope with nonlinear systems by employing input-output data based on the original mathematical description of the system. Fuzzy rules, which are determined based on the designer's knowledge on the system nonlinear dynamics are *if-then* fuzzy sets, logic, and inference. These rules play a fundamental role in representing a proficient control knowledge in linking the input variables of the fuzzy controllers to the output variable (or variables). Two major types of fuzzy control techniques are categorized into the Mamdani and Takagi–Sugeno fuzzy rules [34]. In this article, the Mamdani FC is employed to improve the inertial response. FC techniques as a powerful adaptive control method based on online measurement represent a faster response against control techniques that require a more time-consuming calculations. This leads to a higher inertia response in CIRES-based system.

A. Mamdani FC Input/Outputs

As mentioned, a suitable performance of an FC system is achieved by an accurate study of input behaviors. The main dynamics, which can impact the inertial response, are selected in this article based on the $\Delta\delta, \omega_m$, and $\dot{\omega}_m$. The correction term u_P, as the output of the FC, adds a power adjustment signal to the governor's output power to support the inertia response of the VSG.

According to the specification of inputs within disturbances, the fuzzy rules are logically expanded as illustrated in Fig. 5. Voltage angle deviation (VAD) of CIRESs with respect to the angle of the steady state is introduced to generalize the rotor angle deviation security constraint for the multi-VSG MG applications. Unlike a SG, in the VSGs, the electromotive force, armature resistance, and synchronous reactance are not defined [22]. Hence, the rotor angle of a VSG is not available to be used in stability considerations. However, the difference between the voltage angle of a generating node with respect to a reference angle for nominal operating point can be employed to keep the VAD criterion for transient stability instead of the rotor angle deviation of SGs. Maximum allowable for VAD is selected as

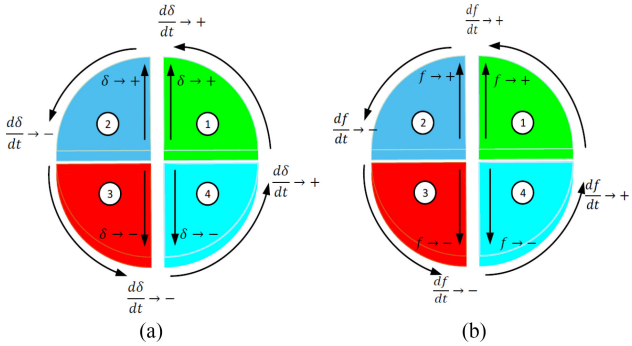

Fig. 5. Specification of (a) the voltage angle δ and (b) the voltage frequency under a perturbation used in the fuzzy-set rules control.

70° for rotor angle deviation [35]. In addition, by employing the situation of frequency and RoCoF, acceleration and deceleration modes can be diagnosed by the fuzzy rules, which tune the injected power, and consequently, the systems inertia during transients. In Fig. 5(a), the variation of δ and its derivative (ω), and in Fig. 5(b) the variation of ω and its derivative (RoCoF), are described and the significant deviation zone of the responses is determined into four sectors such that the quantity in each sector can be one of PQ (i.e., positive quantity, implies upper deviation), ZE (i.e., zero, implies usual quantity), or NQ (i.e., negative quantity, implies less deviation). To improve the inertial response, the rules are implemented such that in Zones 1 and 3, where the frequency response deviates from its nominal value (such as massive load changes or islanding after a fault), u_P adjusts a large input power of the swing equations by reducing the stress of the governor power. On the other hand, in Zones 2 and 4, where the frequency response is perverting towards the nominal value, a low amount of the active power is injected through the control input u_p, as shown in Fig. 6.

B. Mechanism and Implementation

Fig. 6 shows the proposed FC-VSG control. The basic VSG control consists of virtual swing equation, the governor model, $Q - V$ droop, measurement and power calculation unit, and voltage reference generator. Voltage and current are measured from the output filter to calculate the active and reactive powers, i.e., P_e and Q_e. A PLL is employed to measure the grid frequency ω_g, which is used in (7) in an error term of $\omega_m - \omega_g$. The main reason for feeding back ω_g is closing the frequency control loop in order to decrease the frequency error, i.e., $\omega_m - \omega_g$ and attenuate the disturbance effect. The governor generates the reference power for (7) according to the nominal power P_0 and the $P - \omega$ droop expressed by (13), where ω_0 is the nominal frequency and k_p is the governor droop gain. On the other hand, the reference voltage generator block, by obtaining the reference voltage from $Q - V$ droop and δ, produces the pulsewidth modulation m_d for the converter switches. Furthermore, to do a more rapid power injection, a high-bandwidth single-loop predictive controller [36] can be applied. The proposed FC modifies the active power only in transient times with u_p as shown in Fig. 6, where the proposed FC unit adjusts the governors output power, i.e., the swing equation input power P_in, then (7) generates ω_m.

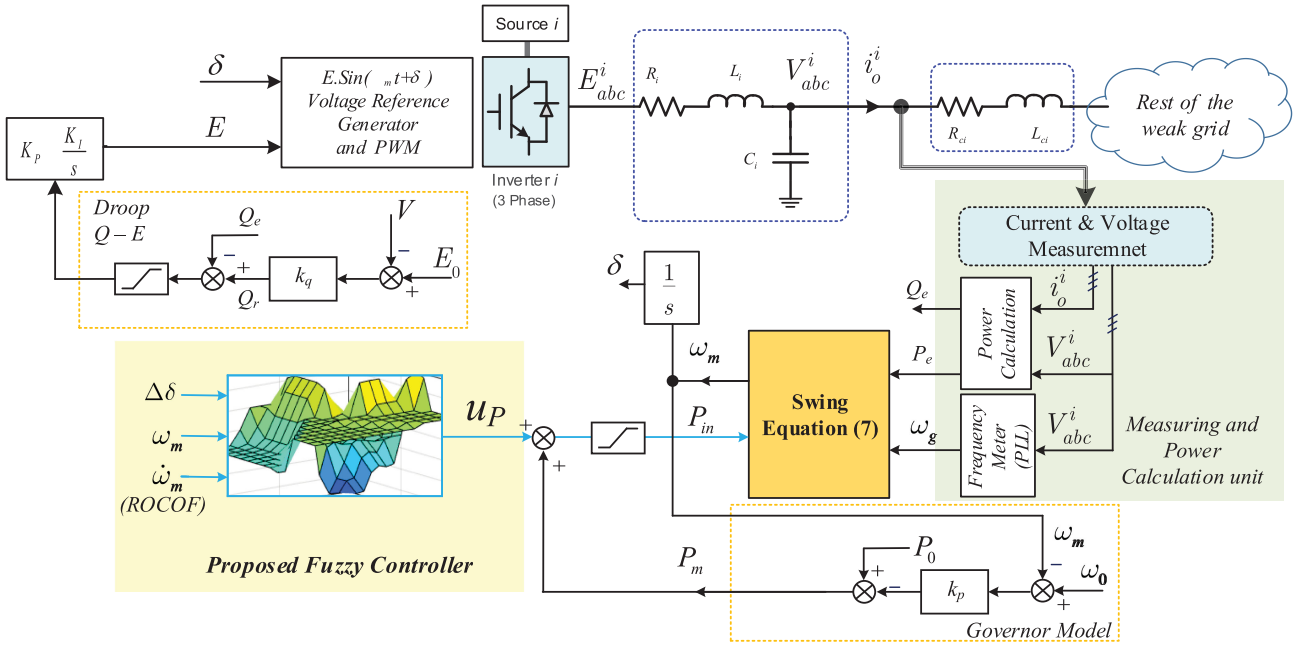

Fig. 6. Proposed FC-VSG control scheme of a CIRES.

TABLE I
EXPANDED FUZZY RULES BY TRAINING DATA

Membership Function			Range	Unit
Fuzzy Inputs	$\Delta\delta$	NQ	nan - (-0.0084) (-0.006)	rad
		ZE	(-0.006) - (0.00227) - (0.00582)	
		PQ	(0.00227) - (0.00582) - (nan)	
	ω	NQ	(49.9) (49.99) (50.04)	Hz
		ZE	(50.03) (50.08) (50.13)	
		PQ	(50.12) (50.26) (50.35)	
	$\dot{\omega}$	NQ	(nan) - (-10.59) - (-5.168)	Hz/s
		ZE	(-5.253) (0.173) (5.599)	
		PQ	(5.572) (11 16.43) - (nan)	
Output	u_P	NQ	(nan)-(-0.004278)- (-7.778e-05)	pu
		ZE	(-0.0001) (0.0041) (0.0083)	
		PQ	(0.008189) (0.01239) (nan)	

In the proposed fuzzy control method, in order to have a closed-loop frequency control, the grid frequency is fed back using a PLL. Although the PLL may cause instability for specific operating points or disturbances, in the normal PLL operation, the frequency feedback to the virtual swing equation improves the performance, i.e., decreases the frequency error signal and attenuates the disturbances. In fact, according to the term of frequency error ($\omega_m - \omega_g$) existing in the virtual swing equation (7), the control method tries to decrease the difference between the control and the grid frequencies.

The characteristics of the input/output membership functions (MFs) such as the type of MFs and the training data ranges are specified in Table I. A proper selection of fuzzy rules has an impressive influence on the performance of the proposed FC and consequently plays an important role in modifying the transient state of the frequency and improving the inertial response. The suitable performance is achieved when the FC modifies P_{in} by the scheduled MFs. Thus, according to the FC input specifications given within the events or disturbances, the fuzzy rules are logically expanded as given in Table I.

V. SIMULATION STUDIES

In order to show the effectiveness of the proposed method, an investigation between the proposed FC-VSG method with the self-tuning optimization based inertia and damping control technique is done. Fig. 7 shows the control diagram of the proposed FC-VSG and the self-tuning adaptive algorithm [20]. The self-tuning VSG continuously search for optimal values of J and D during the utilization of the VSG to minimize the RoCoF and frequency nadir of the system.

As it can be seen in the self-tuning method, the adaptive block continuously searches and optimizes the VSG parameters based on the following cost function:

$$\begin{aligned}
\min \quad & \mathrm{C} = \gamma_1 \left(\frac{d\omega}{dt_{k+1}}\right)^2 + \gamma_2 (J_{k+1})^2 + \gamma_3 (e_{k+1})^2 \\
& + \gamma_4 (D_{k+1})^2 \\
\text{subject to: if} \quad & \left\{ (|e_k| \geq \varepsilon) \ \text{and} \ \left(e_k \frac{d\omega}{dt_k} \leq 0 \right) \right\} \\
& (J, D) \in U_J \times U_D \\
& \gamma_1, \gamma_2, \gamma_3, \gamma_4 > 0 \\
\text{else} \quad & (J, D) \in \emptyset \times U_D \\
& \gamma_1 = \gamma_2 = 0, \gamma_{3,4} > 0
\end{aligned} \tag{14}$$

where $\gamma_1 - \gamma_4$ are the design parameters, $e_k = \omega_0 - \omega$, subscript $k+1$ shows the predicted value for the next time step, and superscript * indicates the optimal value. More details are explained in [20].

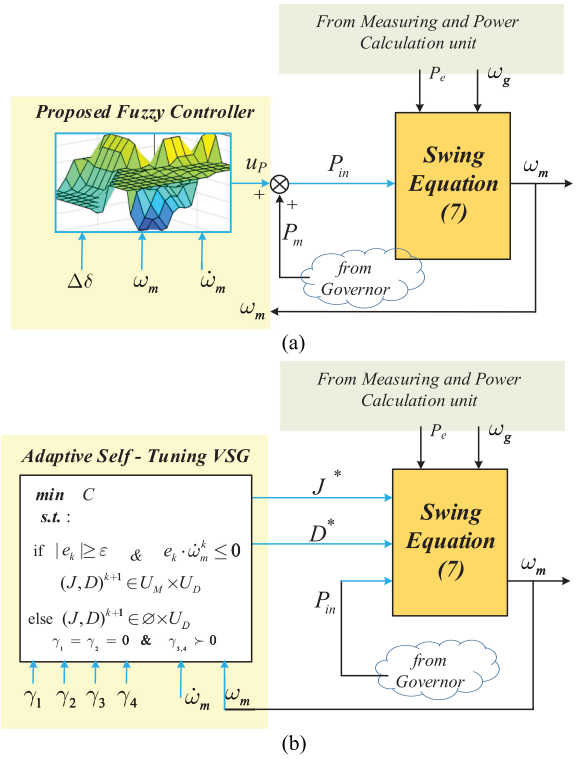

Fig. 7. Control block diagrams of the proposed FC-VSG versus the existing self-tuning VSG control scheme [20].

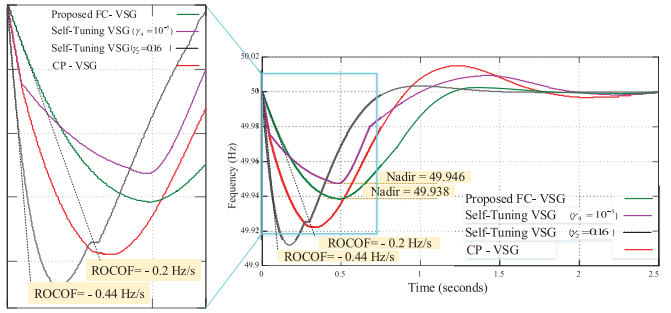

Fig. 8. Simulation result to compare the proposed FC-VSG versus self-tuning VSG control schemes and a constant parameter VSG.

TABLE II
ELECTRICAL AND CONTROL PARAMETERS FOR THE SIMULATION AND EXPERIMENTAL SYSTEMS

Electrical Parameters		
Parameters	Symbol	Value
Output voltage of rectifier	V_{DC}	650 V
Nominal voltage magnitude	V_i	325 V
Nominal Frequency	f	50 Hz
Switching Frequency	f_s	10 kHz
Capacitance of LCL filter	C_f	25 μ F
Input / output inductance of LCL filter	L_i / L_o	1.8 mH
Load 1	Z_1	43 Ω , 0.3 H
Load 2	Z_2	124 Ω , 0.1 H
VSG Inner Loop Coefficients and other Control Parameters		
Control Parameters	Symbol	Value
Governor droop coefficient	k_p	0.0025 pu
Q-v droop coefficient	k_q	0.0125 pu
Apparant power	S_{base}	10 kVA
Moment of inertia	$(J\omega_0^2)/S_{base}$	8 s
Damping coefficient	$(D\omega_0)/S_{base}$	17 pu

It is worth to highlight that in bang–bang adaptive methods, the control part selects appropriate inertia and damping coefficients from a finite set of J and D. However, this approach is fast enough to support the inertia response, but it leads the system to have a finite combination of optional states predefined by the algorithm. The self-tuning adaptive method, as a modified design of the bang–bang adaptive method, selects also the appropriate inertia and damping coefficients from a finite set but with respect to a cost function. The selection will be done after a minimizing the cost function over the finite set by employing the frequency prediction. The main issue in this self-tuning adaptive method is its time-consuming feature due to: 1) calculation and time consumption of the frequency prediction, and 2) calculation and time consumption to minimize the cost function and select the optimal inertia and damping coefficients. It will be worse by increasing the elements of the finite set $U_J \times U_D$.

Fig. 8 shows the simulation results where comparing of the proposed fuzzy VSG (FC-VSG) controller with the self-tuning VSG (ST-VSG) and a conventional VSG controller having constant parameters (CP-VSG) are illustrated. The load increases by 0.2 kW at $t = 0$ s. After load change, and consequently the frequency deviation, as a secondary control is applied, the frequency restores to its nominal value, i.e., 50 Hz. The RoCoF and frequency nadir values can be observed for all wave forms. Two different wave forms are shown for the ST-VSG control, where the impact of the design parameters γ_1, γ_2, γ_3, and γ_4 were highlighted. The initial state of the inertia and damping coefficients are selected as the same as their maximum values as it is shown in Table II. Although, the frequency nadir in the ST-VSG can result in a lower value by appropriate selecting the design parameters (in magenta color), the inertial response of the proposed FC-VSG leads to a lower RoCoF and a desired frequency nadir by changing the input power (P_{in}) by the FC-VSG after disturbances. Note that the undesired selection of the design parameters can even cause the worse inertial response (in black color) than the CP-VSG.

VI. EXPERIMENTAL VERIFICATION

To assess the effectiveness and appropriate performance of the proposed FC-VSG, experimental tests are performed on the prototype set up shown in Fig. 9. A three-phase grid-connected converter, programmed as VSG, with a lower scale voltage and power ratings, is employed to implement the control platform. The FC-VSG control platform is coded from MATLAB/Simulink environment to the DS1007 dSPACE system by its control desk space. The DS2004 analog-digital board is used to collect the voltage and current measurements into the dSPACE. The phase angle of the PCC voltage and the grid voltage is detected by the PLL. A rectifier having a constant dc voltage supply is used at the dc side. In the grid connected mode, grid simulator Chroma 61850 with power rating 45 kVA is employed to generate the grid voltage. Other control and electrical parameters are given in Table II.

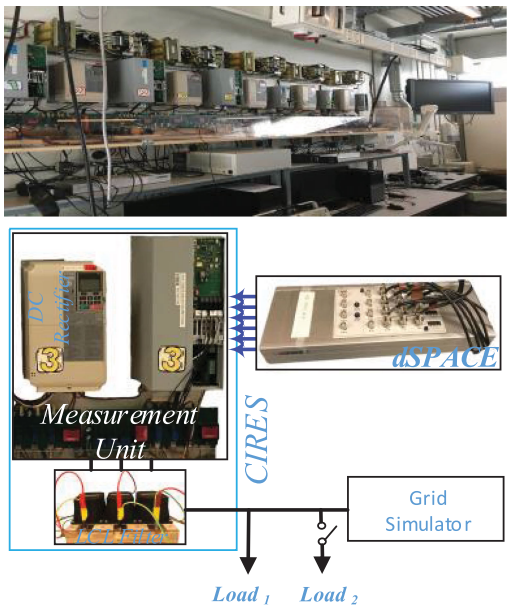

Fig. 9. Laboratory setup for experimented tests.

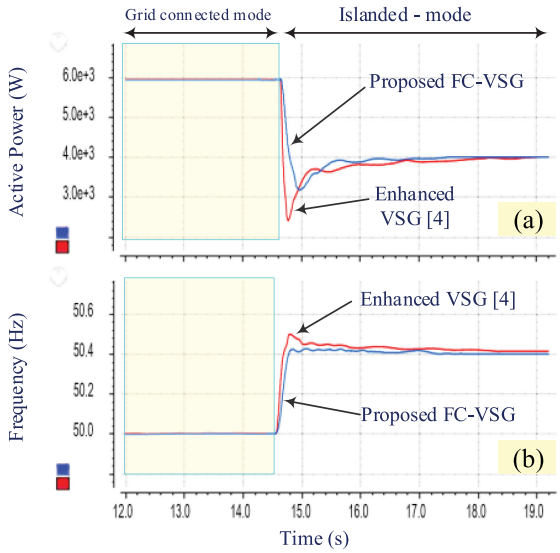

Fig. 10. Experimental results. (a) Active power. (b) Frequency response for Scenario 1: Intentional islanding.

To further verify and prove the effectiveness and merits of the suggested FC-VSG, it is compared with the presented method in [4]. Without loss of generality, consider a CIRES, which is connected to the grid. Following, to show the merits of the proposed FC-VSG, two scenarios are considered: Intentional islanding and load step.

A. Scenario 1: Intentional Islanding

In this scenario, the goal is to show the improved performance of inertial response of the proposed FC-VSG over the existing VSG control approaches. The reference values for the P_0, Q_0, and E_0 are selected as the same as given in [4]. Fig. 10(a) and (b) illustrates the inertial response of a CIRES through the active power and the frequency compared with the enhanced VSG [4] under an intentional islanding event at $t = 14.6$ s. The overshoot of the proposed FC-VSG and enhanced VSG controllers are as 0.42 and 0.48 Hz, respectively. Their RoCoF are 2 and 4 Hz/s, respectively. Therefore, one can conclude the inertial response improvement is obtained according to the overshoot and RoCoF values.

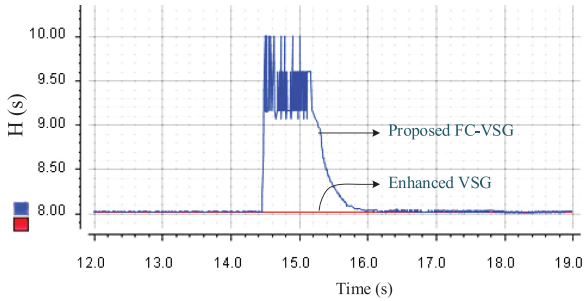

Fig. 11. Experimental results: Moment of inertia monitoring for Scenario 1: Intentional islanding.

Fig. 11 shows the moment of inertia of the closed-loop system including the basic VSG controller and the supplementary fuzzy controller, which can be calculated from (7) by finding the moment of inertia as follows:

$$J = \frac{P_m + u_p - P_e - D(\omega_m - \omega_g)}{\omega_m \dot{\omega}_m}. \tag{15}$$

It is obvious that the moment of inertia is increased adaptively in the transients caused by intentional islanding. It is due to the performance of the employed fuzzy controller. In fact both the conventional VSG approach [3] and the enhanced VSG approach [4] are not able to improve the inertial response in an islanding operation.

After the islanding process, since the local load is lower than the power set point, the governor mechanism tunes the system frequency in steady state based on the consumed power at the connected loads.

B. Scenario 2: Load Step

In this scenario, the effectiveness of the proposed FC-VSG to a load change as a common disturbance in islanded mode is investigated. As shown in Fig. 12(a) and (b), a load change happens at $t = 8$ s, and the active power is increased from 6 to 9 kW, and consequently the frequency is drooped from 50 to 49.4 Hz. The frequency nadir of the proposed FC-VSG and enhanced VSG controllers are as 0.60 and 0.62 Hz, respectively. Their RoCoF is -3 and -6 Hz/s, respectively. Therefore, the inertial response is improved by the proposed FC-VSG controller with respect to the enhanced VSG controller [4] according to the frequency nadir and RoCoF values. Note that decreasing the rate of active power is equivalent to the lower RoCoF, which means improving inertial response.

Fig. 13 shows the moment of inertia of the closed-loop system including the basic VSG controller and the supplementary fuzzy controller, which can be calculated using (15). It can be shown that the moment of inertia is increased adaptively during

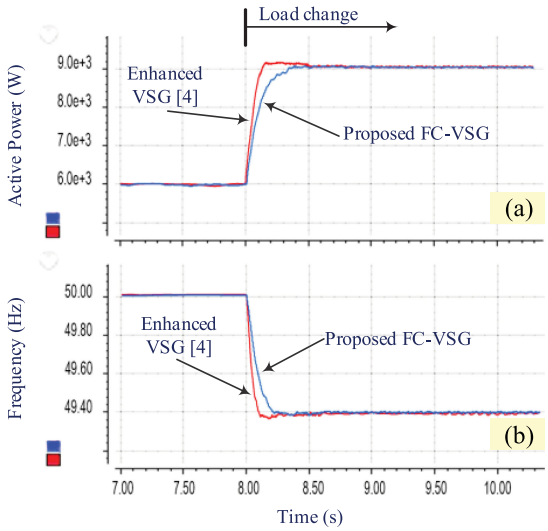

Fig. 12. Experimental results. (a) Active power. (b) Frequency response for Scenario 2: Load step.

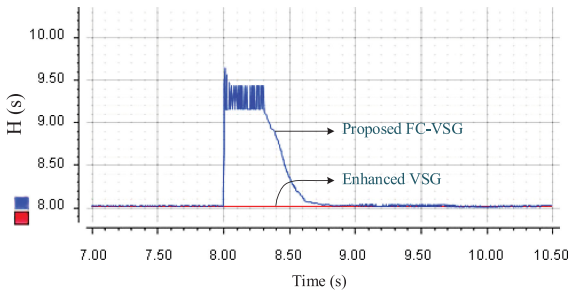

Fig. 13. Experimental results: Moment of inertia monitoring for Scenario 2: Load step.

transients of the load changing. Note that the inertia increase is due to the performance of the embedded fuzzy controller on the basic VSG controller.

It is noteworthy that the injected virtual inertia to the grid by the proposed FC-VSG control can be remarkable in the grid-connected MG mode when a considerable number of ac MGs supported by FC- controlled VSG are connected to the upstream grid.

VII. Conclusion

In this article, an FC-VSG control method is proposed as a communication-less control method to improve the inertial response for CIRES-based autonomous MGs. First, the inertia support necessity in grid connected CIRESs is highlighted. The main idea of the proposed FC-VSG is developed based on the transient control function, which applied to the swing equation's input power, the injected governor power, in order to increase the inertial response. Adjustment of the governor's power to increase the inertia is realized in an FC platform by employing variation the voltage angle, frequency, and RoCoF. To highlight the effectiveness of the online measurement techniques such as FC to support the inertia response, a comparison with a self-tuning optimization-based techniques is done. Furthermore, experimental verification is demonstrated where the proposed FC-VSG achieves desirable transient and inertial performance, and keeps the RoCoF support feature for CIRES-based MGs. Experimental results imply that the proposed FC-VSG is able to do islanding and handle the loading transition disturbances rapidly, without oscillations and also obtain a better inertial response. Even when an islanding event as a large disturbance occurs, the overshoot is suppressed due to the increased system damping.

References

[1] H. Bevrani, *Robust Power System Frequency Control*, 2nd ed. New York, NY, USA: Springer, 2014.
[2] H. Bevrani, B. François, and T. Ise, *Microgrid Dynamics and Control*. Hoboken, NJ, USA: Wiley, 2017.
[3] C. Yuan, C. Liu, X. Zhang, T. Zhao, X. Xiao, and N. Tang, "Comparison of dynamic characteristics between virtual synchronous generator and droop control in inverter-based distributed generators," *IEEE Trans. Power Electron.*, vol. 31, no. 5, pp. 3600–3611, May 2016.
[4] J. Liu, Y. Miura, H. Bevrani, and T. Ise, "Enhanced virtual synchronous generator control for parallel inverters in microgrids," *IEEE Trans. Smart Grid*, vol. 8, no. 5, pp. 2268–2277, Sep. 2017.
[5] H. Bevrani, T. Ise, and Y. Miura, "Virtual synchronous generators: A survey and new perspectives," *Int. J. Electric. Power Energy Syst.*, vol. 54, pp. 244–254, 2014.
[6] F. Milano, F. Dörfler, G. Hug, D. J. Hill, and G. Verbič, "Foundations and challenges of low-inertia systems," in *Proc. IEEE Power Syst. Comput. Conf.*, Aug. 2018, pp. 1–25.
[7] T. Shintai, Y. Miura, and T. Ise, "Oscillation damping of a distributed generator using a virtual synchronous generator," *IEEE Trans. Power Del.*, vol. 29, no. 2, pp. 668–676, Apr. 2014.
[8] J. Rocabert, A. Luna, F. Blaabjerg, and P. Rodriguez, "Control of power converters in ac microgrids," *IEEE Trans. Power Electron.*, vol. 27, no. 11, pp. 4734–4749, Nov. 2012.
[9] S. A. Khajehoddin, M. Karimi-Ghartemani, and M. Ebrahimi, "Grid-supporting inverters with improved dynamics," *IEEE Trans. Ind. Electron.*, vol. 66, no. 5, pp. 3655–3667, May 2019.
[10] H. Wu *et al.*, "Small-signal modeling and parameters design for virtual synchronous generators," *IEEE Trans. Ind. Electron.*, vol. 63, no. 7, pp. 4292–4303, Jul. 2016.
[11] F. Wang, L. Zhang, X. Feng, and H. Guo, "An adaptive control strategy for virtual synchronous generator," *IEEE Trans. Ind. Appl.*, vol. 54, no. 5, pp. 5124–5133, Sep./Oct. 2018.
[12] H. Xu, X. Zhang, F. Liu, R. Shi, C. Yu, and R. Cao, "A reactive power sharing strategy of VSG based on virtual capacitor algorithm," *IEEE Trans. Ind. Electron.*, vol. 64, no. 9, pp. 7520–7531, Sep. 2017.
[13] U. Markovic, Z. Chu, P. Aristidou, and G. Hug-Glanzmann, "LQR-based adaptive virtual synchronous machine for power systems with high inverter penetration," *IEEE Trans. Sustain. Energy*, vol. 10, no. 3, pp. 1501–1512, Jul. 2019.
[14] A. Asrari, M. Mustafa, M. Ansari, and J. Khazaei, "Impedance analysis of virtual synchronous generator-based vector controlled converters for weak ac grid integration," *IEEE Trans. Sustain. Energy*, vol. 10, no. 3, pp. 1481–1490, Jul. 2019.
[15] S. D'Arco and J. A. Suul, "Virtual synchronous machines classification of implementations and analysis of equivalence to droop controllers for microgrids," in *Proc. IEEE Grenoble Conf.*, 2013, pp. 1–7.
[16] O. Mo, S. D'Arco, and J. A. Suul, "Evaluation of virtual synchronous machines with dynamic or quasi-stationary machine models," *IEEE Trans. Ind. Electron.*, vol. 64, no. 7, pp. 5952–5962, Jul. 2017.
[17] Y. Cao *et al.*, "A virtual synchronous generator control strategy for VSC-MTDC systems," *IEEE Trans. Energy Convers.*, vol. 33, no. 2, pp. 750–761, Jun. 2018.
[18] J. Fang, G. Xiao, X. Yang, and Y. Tang, "Parameter design of a novel series-parallel-resonant LCL filter for single-phase half-bridge active power filters," *IEEE Trans. Power Electron.*, vol. 32, no. 1, pp. 200–217, Jan. 2017.
[19] D. Li, Q. Zhu, S. Lin, and X. Bian, "A self-adaptive inertia and damping combination control of VSG to support frequency stability," *IEEE Trans. Energy Convers.*, vol. 32, no. 1, pp. 397–398, Mar. 2017.

[20] M. A. Torres L, L. A. Lopes, L. A. Moran T, and J. R. Espinoza C, "Self-tuning virtual synchronous machine: A control strategy for energy storage systems to support dynamic frequency control," *IEEE Trans. Energy Convers.*, vol. 29, no. 4, pp. 833–840, Dec. 2014.
[21] J. Alipoor, Y. Miura, and T. Ise, "Power system stabilization using virtual synchronous generator with alternating moment of inertia," *IEEE J. Emerg. Sel. Topics Power Electron.*, vol. 3, no. 2, pp. 451–458, Jun. 2015.
[22] J. Alipoor, T. Ise, and Y. Miura, "Stability assessment and optimization methods for microgrid with multiple VSG units," *IEEE Trans. Smart Grid*, vol. 9, no. 2, pp. 1462–1471, Mar. 2018.
[23] N. Soni, S. Doolla, and M. C. Chandorkar, "Improvement of transient response in microgrids using virtual inertia," *IEEE Trans. Power Del.*, vol. 28, no. 3, pp. 1830–1838, Jul. 2013.
[24] D. K. Dheer, N. Soni, and S. Doolla, "Improvement of small signal stability margin and transient response in inverter-dominated microgrids," *Sustain. Energy, Grids Netw.*, vol. 5, pp. 135–147, 2016.
[25] S. Zhang, Y. Mishra, and M. Shahidehpour, "Fuzzy-logic based frequency controller for wind farms augmented with energy storage systems," *IEEE Trans. Power Syst.*, vol. 31, no. 2, pp. 1595–1603, Mar. 2015.
[26] J. Fang, H. Li, Y. Tang, and F. Blaabjerg, "Distributed power system virtual inertia implemented by grid-connected power converters," *IEEE Trans. Power Electron.*, vol. 33, no. 10, pp. 8488–8499, Oct. 2018.
[27] A. Karimi, Y. Khayat, M. Naderi, R. Mirzaee, and H. Bevrani, "Improving transient performance of VSG based microgrids by virtual facts'functions," in *Proc. IEEE Smart Grid Conf.*, Mar. 2017, pp. 1–6.
[28] A. Ulbig, T. S. Borsche, and G. Andersson, "Impact of low rotational inertia on power system stability and operation," *IFAC Proc. Vol.*, vol. 47, no. 3, pp. 7290–7297, 2014.
[29] N. Miller, D. Lew, and R. Piwko, "Technology capabilities for fast frequency response," *GE Energy Consulting, Tech. Rep.*, 2017.
[30] F. Statnett, "Challenges and opportunities for the nordic power system," Tech. Rep., 2016.
[31] ERCOT, "Future ancillary services in ERCOT," Tech. Rep., 2013.
[32] M. Naderi, Y. Khayat, Q. Shafiee, H. Bevrani, and F. Blaabjerg, "Modeling of islanded microgrids using static and dynamic equivalent Thevenin circuits," in *Proc. 20th Eur. Conf. Power Electron. Appl.*, 2018, pp. 1–10.
[33] J. M. Guerrero, J. Matas, L. G. De Vicuña, N. Berbel, and J. Sosa, "Wireless-control strategy for parallel operation of distributed generation inverters," in *Proc. IEEE Int. Symp. Ind. Electron.*, 2005, vol. 2, pp. 845–850.
[34] H. Ying, *Fuzzy Control and Modeling: Analytical Foundations and Applications*. Hoboken, NJ, USA: Wiley, 2000.
[35] Q. Jiang, Y. Wang, and G. Geng, "A parallel reduced-space interior point method with orthogonal collocation for first-swing stability constrained emergency control," *IEEE Trans. Power Syst.*, vol. 29, no. 1, pp. 84–92, Jan. 2013.
[36] T. Dragičević, "Model predictive control of power converters for robust and fast operation of ac microgrids," *IEEE Trans. Power Electron.*, vol. 33, no. 7, pp. 6304–6317, Jul. 2018.

Amin Karimi received the B.E. degree in electrical engineering from Educational Research Complex of Isfahan, Tehran, Iran, in 2005, and the M.Sc. degree in analog electronic engineering from Razi University, Kermanshah, Iran, in 2009. He is currently working toward the Ph.D. degree in control of power systems at University of Kurdistan, Sanandaj, Iran.

His current research interests include power electronics, virtual inertia, and robust/intelligent control.

Yousef Khayat (S'16) received the B.Sc. degree from Urmia University, Urmia, Iran, in 2012, and the M.Sc. (Hons.) degree from the Iran University of Science and Technology, Tehran, Iran, in 2014, both in electrical engineering. He is currently working toward the Ph.D. degree in control of power systems at the University of Kurdistan, Sanandaj, Iran. He is also currently a Ph.D. Visiting Student with Aalborg University, Aalborg, Denmark.

His research interests include microgrid dynamics and control, robust, predictive, and nonlinear control for application of power electronics in distributed systems.

Mobin Naderi (S'16) was born in Paveh, Iran. He received the B.Sc. degree from Tabriz University, Tabriz, Iran, in 2012, and the M.Sc. degree from Iran University of Science and Technology, Tehran, Iran, in 2014, both in electrical engineering. He is currently working toward the Ph.D. degree in the control of power systems at the University of Kurdistan, Sanandaj, Iran. He is also currently a Ph.D. Visiting Student with Aalborg University, Aalborg, Denmark.

His research interests include robust control, microgrid stability and control, and ac networked microgrids.

Tomislav Dragičević (S'09–M'13–SM'17) received the M.Sc. and industrial Ph.D. degrees in electrical engineering from the Faculty of Electrical Engineering, Zagreb, Croatia, in 2009 and 2013, respectively.

From 2013 to 2016, he was a Postdoctoral Research Associate with Aalborg University, Denmark. From March 2016, he is an Associate Professor with Aalborg University, Denmark, where he leads an Advanced Control Lab Advanced Control Lab. He made a Guest Professor stay at Nottingham University, U.K. during Spring/Summer of 2018. He has authored and coauthored more than 155 technical papers (more than 70 of them are published in international journals, mostly IEEE transactions) in his domain of interest as well as, eight book chapters and a book in his field of study. His research interests include design and control of microgrids and application of advanced modeling and control concepts to power electronic systems.

Dr. Dragičević is a recipient of the Koncar Prize for the Best Industrial Ph.D. Thesis in Croatia and a Robert Mayer Energy Conservation Award. He is an Associate Editor for the IEEE TRANSACTIONS ON INDUSTRIAL ELECTRONICS, IEEE EMERGING AND SELECTED TOPICS IN POWER ELECTRONICS, and IEEE INDUSTRIAL ELECTRONICS MAGAZINE.

Rahmatollah Mirzaei received the B.E. degree in electronic engineering from Tabriz University, Tabriz, Iran, in 1987, the M.Sc. degree in control engineering from Tehran University, Tehran, Iran, in 1991, and the Ph.D. degree in power electronics from the Indian Institute of Science, Bengaluru, India, in 2007.

He is currently an Assistant Professor and a member of the Smart/Micro Grids Research Center with the University of Kurdistan, Sanandaj, Iran, where he was a Lecturer since 1993. His research interests include design, analysis, control, and modeling of power converters for PFC circuits, soft switching, and active filter systems.

Frede Blaabjerg (S'86–M'88–SM'97–F'03) received the Ph.D. degree in electrical engineering from Aalborg University, Aalborg, Denmark, in 1995.

He was with ABB-Scandia, Randers, Denmark, from 1987 to 1988. He became an Assistant Professor in 1992, an Associate Professor in 1996, and a Full Professor of power electronics and drives in 1998. In 2017, he became a Villum Investigator. He is *honoris causa* with the University Politehnica Timisoara, Romania, and Tallinn Technical University, Estonia. He has authored and Co-Authored more than 600 journal papers in the fields of power electronics and its applications. He is the Co-Author of four monographs and editor of ten books in power electronics and its applications. His current research interests include power electronics and its applications such as in wind turbines, PV systems, reliability, harmonics, and adjustable speed drives.

Prof. Blaabjerg is the recipient of 30 IEEE Prize Paper Awards, the IEEE PELS Distinguished Service Award in 2009, the EPE-PEMC Council Award in 2010, the IEEE William E. Newell Power Electronics Award 2014, and the Villum Kann Rasmussen Research Award 2014. He was the Editor-in-Chief of the IEEE TRANSACTIONS ON POWER ELECTRONICS, from 2006 to 2012. He was the Distinguished Lecturer for the IEEE Power Electronics Society from 2005 to 2007 and for the IEEE Industry Applications Society from 2010 to 2011 as well as from 2017 to 2018. From 2019 to 2020, he is the President of IEEE Power Electronics Society. He is the Vice-President of the Danish Academy of Technical Sciences too. He is nominated in 2014–2018 by Thomson Reuters to be between the 250 most cited researchers in engineering in the world.

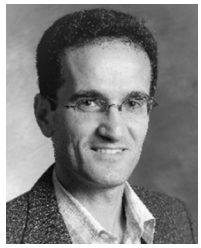

Hassan Bevrani (S'90–M'04–SM'08) received the Ph.D. degree in electrical engineering from Osaka University, Suita, Japan, in 2004.

He is currently a Full Professor, the Program Leader of Micro/Smart Grids Research Center, and the Vice Chancellor for Research at the University of Kurdistan. Over the years, he has worked with Osaka University, Kumamoto University, Japan, Queensland University of Technology, Australia, Kyushu Institute of Technology, Centrale Lille, France, and the Technical University of Berlin, Germany. He is the author of six international books, 15 book chapters, and more than 300 journal/conference papers. His current research interests include smart grid operation and control, power system stability, microgrid dynamics and control, and intelligent/robust control applications in power electric industry.